Proposal for a Study of Ionization Cooling of a Low-Energy Muon Beam by LH_2 and LiH Absorbers

C.-X. Wang
Argonne National Laboratory, Argonne, IL 60439

D.B. Cline, Y. Fukui, K. Lee, Y. Pischalnikov
University of California Los Angeles, Los Angeles, CA 90095

K.-J. Kim, M.J. Oreglia
University of Chicago, Chicago, IL 60637

G.G. Hanson
Indiana University, Bloomington, IN 47405

C. Lu, K.T. McDonald, E.J. Prebys
Princeton University, Princeton, NJ 08544

T.R. Edgecock, J.R.J. Bennett
Rutherford Appleton Laboratory, Chilton, Didcot, Oxon, UK OX11 0QX

(July 5, 2000)

Abstract

As a step in a larger program of muon cooling R&D, we propose to study ionization cooling of 170-MeV/c muons in LH_2 and LiH absorbers inside a 2-2.5 T solenoid magnet but without rf acceleration ("minicooling"). The required flux of muons is small, such that only one muon is in the apparatus at a time; the desired muon bunch will be reconstructed offline via software. This study will validate the analytic and numerical calculations of ionization cooling via measurements of multiple scattering and straggling, will demonstrate transverse cooling of a muon bunch including the predicted coupling of transverse emittance to angular momentum when inside a solenoid channel, and will use diagnostics suitable for further cooling studies. The proposed demonstration of transverse cooling via the single-particle method is a natural extension of TRIUMF E875 that is making a precision measurement of muon multiple scattering in low-Z absorbers.

1 Introduction

As has been noted since the earliest discussions of storage rings, "cooling" of the beam emittance is the key to a practical device [1]. In the case of muon storage rings, the cooling must be accomplished in a time of order 1 μs to avoid loss of the beam by muon decay. This excludes such relatively slow methods as stochastic cooling, electron cooling and radiative cooling. When charged particles pass through matter they lose energy to the medium via excitation and ionization of atomic electrons. This technique of ionization cooling [1, 2] is uniquely applicable to muon beams because the interaction of the muons with the atomic nuclei is negligible. Ionization cooling is critical to the success of both muon colliders [3] where a reduction of 6-dimensional phase volume by a factor of 10^6 is desired, and to neutrino factories based on muon storage rings [4, 5, 6] where a reduction factor of 10-100 is desired. However, ionization cooling of muons has not yet been demonstrated in the laboratory.[1]

The present proposal is to study the basic principles of ionization cooling of muons by low-Z absorbers, including the effect of a solenoid magnetic field which couples transverse emittance to canonical angular momentum.

We first review the principles of ionization cooling in sec. 1.2, and then place the present proposal in a larger context of studies of ionization cooling in sec. 1.2. Etc.....

1.1 Analytic Expressions for Ionization Cooling

If there were no fluctuations in the interaction of muons with atoms, perfect cooling could be achieved simply by removing all of the muons' initial kinetic energy and momentum, and reaccelerating the muons to their initial energy via rf cavities. However, the processes of multiple scattering and energy straggling "heat" the muons and make the cooling process less efficient. This implies that the muons must lose and regain several times their initial energy in a practical ionization cooling channel. The rf acceleration costs will therefore be higher for higher energy muons. The present view is that ionization cooling of muons is most practical for beams of central momentum about 180 MeV/c.

While energy loss to ionization in a medium reduces all components of a muon's momentum, the longitudinal momentum spread of a low-momentum beam (< 300 MeV/c) is actually increased because lower momentum muons lose more momentum than higher momentum muons. Therefore, ionization cools only transverse momentum, and it is useful to discuss transverse and longitudinal emittance separately.

1.2 Transverse Emittance

We first consider the 2-d normalized transverse emittance $\epsilon_{\perp,N}$ defined by

$$m^2c^2\epsilon_{\perp,N}^2 = \left\langle x^2 \right\rangle \left\langle P_x^2 \right\rangle - \left\langle xP_x \right\rangle^2 , \tag{1}$$

where x is a transverse spatial coordinate of a bunch of muons propagating along the z axis, and E and P are the energy and momentum. To obtain a relatively simple analytic

[1] The IGISOL technique [7] for production of radioactive beam involves a step in which heavy ions of energy less than the Coulomb barrier (≈ 3 MeV/nucleon) are stopped in helium gas. This is in effect a form of ionization cooling, although apparently unrecognized as such by its practitioners.

approximation for the rate of change of $\epsilon_{\perp,N}$ as the muons pass through an absorber, we use the impulse approximation that the muons' momenta, but not their positions, are changed by interactions in the absorber. Further, we ignore correlations such as $\langle xP_x \rangle$. With these approximations, there is no difference in the rate of change of the canonical emittance (34) and the mechanical emittance (1). Then,

$$2m^2c^2\epsilon_{\perp,N}\frac{d\epsilon_{\perp,N}}{dz} = \left\langle x^2 \right\rangle \left\langle \frac{dP_x^2}{dz} \right\rangle - 2\left\langle xP_x \right\rangle \left\langle x\frac{dP_x}{dz} \right\rangle \approx \left\langle x^2 \right\rangle \left\langle \frac{dP_x^2}{dz} \right\rangle. \tag{2}$$

In the paraxial approximation, $P_x \approx \theta_x P$, and with neglect of correlations, we have

$$\begin{aligned} \left\langle \frac{dP_x^2}{dz} \right\rangle &\approx \left\langle \theta_x^2 \frac{dP^2}{dz} \right\rangle + \left\langle P^2 \frac{d\theta_x^2}{dz} \right\rangle \approx 2\frac{\langle P_x^2 \rangle}{\beta^2 E}\frac{dE}{dz} + \left\langle P^2 \right\rangle \left\langle \frac{d\theta_x^2}{dz} \right\rangle \\ &\approx 2\frac{\langle P_x^2 \rangle}{\beta^2 E}\frac{dE}{dz} + \frac{(13.6\ \mathrm{MeV}/c)^2}{\beta^2 L_R}, \end{aligned} \tag{3}$$

where L_R is the radiation length of the absorber, and now E, P, and $\beta = v/c = c^2P/E$ represent bunch averages.

We also suppose that $\langle x^2 \rangle$ can be related as

$$\left\langle x^2 \right\rangle = \epsilon_\perp \beta_\perp^\star = \frac{\epsilon_{\perp,N}\beta_\perp^\star}{\gamma\beta}, \tag{4}$$

where $\epsilon_\perp$ is the rms 2-d geometric transverse emittance, and $\beta_\perp^\star$ is the value of the betatron function of the transversely confining beam optics at the position of the absorber.

With all these approximations, the rate of cooling of transverse emittance is

$$\begin{aligned} \frac{d\epsilon_{\perp,N}}{dz} &\approx \frac{\epsilon_{\perp,N}}{\beta^2 E}\frac{dE}{dz} + \frac{\beta_\perp^\star (13.6\ \mathrm{MeV}/c)^2}{2\beta^3 E m_\mu L_R} \\ &\approx \frac{1}{\beta^2 E L_R}\left[-\frac{\pi m_e c^2 \epsilon_{\perp,N}}{\alpha(Z+1)\ln\frac{287}{\sqrt{Z}}}\left(\frac{1}{\beta^2}\ln\frac{2\gamma^2\beta^2 m_e c^2}{I} - 1\right) + \frac{\beta_\perp^\star (13.6\ \mathrm{MeV}/c)^2}{2\beta m_\mu}\right], \end{aligned} \tag{5}$$

where the second form is obtain by use of the Bethe-Bloch formula for dE/dz, given as eq. (23.1) of [28]:

$$\frac{dE}{dz} \approx -4\pi r_e^2 m_e c^2 N_0 \rho \frac{Z}{A}\left(\frac{1}{\beta^2}\ln\frac{2\gamma^2\beta^2 m_e c^2}{I} - 1\right), \tag{6}$$

and of the fit for the radiation length L_R as given in (23.19) of [28]:

$$\frac{1}{L_R} = 4\alpha r_e^2 N_0 \rho \frac{Z(Z+1)}{A}\ln\frac{287}{\sqrt{Z}}. \tag{7}$$

Here, N_0 is Avagadro's number (per mole), ρ is the density of the absorber in, say, g/cm^3, the atomic "weight" A is in g/mole, I is the ionization potential of the absorber material, and α is the fine-structure constant. We have set the maximum kinetic energy imparted to an electron in a collision with a muon to $2\gamma^2\beta^2 m_e c^2$, which is valid for $\gamma m_e/m_\mu \ll 1$, as

holds in the muon cooling channel. We have also neglected the density-effect term, which is significant only for $\gamma \gtrsim 3$.

For example, with a hydrogen absorber we take $I = 15$ eV, and find

$$\frac{d\epsilon_{\perp,N}}{dz} \approx \frac{1}{\beta^2 E L_R}\left[-19.2\epsilon_{\perp,N}\left(\frac{12}{\beta^2}-1\right)+\frac{0.88\beta_\perp^\star}{\beta}\right], \tag{8}$$

where the value 12 holds for $\gamma\beta \approx 2$.

The minimum value of $\epsilon_{\perp,N}$ that can be achieved with a hydrogen absorber at a location where the betatron function is $\beta_\perp^\star$ is then,

$$\epsilon_{\perp,N,\mathrm{min}} = \frac{0.0038\beta\beta_\perp^\star}{1-\beta^2/12}. \tag{9}$$

Equation (8) can be rewritten in terms of $\epsilon_{\perp,N,\mathrm{min}}$ as

$$\frac{1}{\epsilon_{\perp,N}}\frac{d\epsilon_{\perp,N}}{dz} \approx -\frac{230\ \mathrm{MeV}(1-\beta^2/12)}{\beta^4 E L_R}\left(1-\frac{\epsilon_{\perp,N,\mathrm{min}}}{\epsilon_{\perp,N}}\right). \tag{10}$$

For example, with $\gamma = 2$, $\beta = 0.866$, $E = 210$ MeV, $P = 182$ MeV/c, then

$$\frac{1}{\epsilon_{\perp,N}}\frac{d\epsilon_{\perp,N}}{dz} \approx -\frac{1.8}{L_R}\left(1-\frac{\epsilon_{\perp,N,\mathrm{min}}}{\epsilon_{\perp,N}}\right). \tag{11}$$

To cool $\epsilon_{\perp,N}$ from, say, $4\epsilon_{\perp,N,\mathrm{min}}$ to $2\epsilon_{\perp,N,\mathrm{min}}$ would require about $0.6L_R \approx 480$ cm of liquid hydrogen, using (11) with $\langle 1-\epsilon_{\perp,N,\mathrm{min}}/\epsilon_{\perp,N}\rangle \approx 2/3$. I believe ICOOL indicates that about 600 cm would be required.

1.3 Longitudinal Emittance

In the thin absorber limit there is no change in z of a particle as it cross an absorber. So if suffices to consider changes in P_z, or nearly equivalently, in E. More precisely, since the central energy E_0 is nonzero, we consider changes $\Delta E = E - E_0$ and desire an expression for $\langle d(\Delta E)^2/dz\rangle$.

There are two effects to consider: the variation in the mean energy loss with particle energy, and fluctuations about the mean. We calculate these separately, and add them in quadrature. First, a particle of energy E that traverses an absorber of thickness δz has mean energy loss δE_{mean} given by

$$\delta E_{\mathrm{mean}} = \frac{dE}{dz}\delta z \approx \left(\frac{dE_0}{dz}+\Delta E\frac{d^2E_0}{dEdz}\right)\delta z. \tag{12}$$

Then change in ΔE is then

$$\delta(\Delta E)_{\mathrm{mean}} \approx \Delta E\frac{d^2E_0}{dEdz}\delta z. \tag{13}$$

Hence,

$$\frac{d(\Delta E)^2_{\mathrm{mean}}}{dz} \approx 2(\Delta E)^2\frac{d^2E_0}{dEdz}, \tag{14}$$

Second, we consider fluctuations in the energy loss in the absorber. To the first approximation, it suffices to consider this only for the central energy E_0. Using the nomenclature "straggling" for this effect, we have an additional term

$$\frac{d(\Delta E)^2_{\rm straggling}}{dz}. \tag{15}$$

Combining this with (14), we have

$$\frac{d(\Delta E)^2}{dz} \approx 2(\Delta E)^2 \frac{d}{dE}\frac{dE_0}{dz} + \frac{d(\Delta E)^2_{\rm straggling}}{dz}. \tag{16}$$

An accessible discussion of straggling is given in sec. 13.3 of [29], with the key result that

$$\frac{d(\Delta E)^2_{\rm straggling}}{dz} = 4\pi(r_e m_e c^2)^2 N_0 \frac{Z}{A}\rho\gamma^2(1-\beta^2/2) = 2\pi(r_e m_e c^2)^2 N_0 \frac{Z}{A}\rho(\gamma^2+1). \tag{17}$$

This result applies only for "thick" absorbers, which is reasonable for the muon collider where we take the energy away 30 times by ionization loss, although each absorber is only about 5% of a radiation length.

When the muons are later accelerated, ΔE remains constant. Thus, ΔE rather than $\Delta E/E$ should be minimized in the cooling apparatus. Hence, the undesirable "heating" due to straggling is minimized by operating the cooling channel at the lowest possible γ, according to (17).

Equation (17) can be recast in a way that emphasizes the radiation length L_R of the absorber by using the fit (7):

$$\frac{d(\Delta E)^2_{\rm straggling}}{dz} = \frac{\pi(m_e c^2)^2 A(\gamma^2+1)}{2\alpha(Z+1)L_R \ln(287/\sqrt{Z})}. \tag{18}$$

Then, eq. (16) can be written

$$\frac{d(\Delta E)^2}{dz} \approx 2(\Delta E)^2 \frac{d}{dE}\frac{dE_0}{dz} + \frac{\pi(m_e c^2)^2(\gamma^2+1)}{2\alpha(Z+1)L_R \ln(287/\sqrt{Z})}. \tag{19}$$

A sense of the relative importance of the two terms in eq. (16) can be gotten from the Bethe-Bloch formula (6). With $E = \gamma m_\mu c^2$, the leading term in the derivative of (6) with respect to E is

$$\frac{d}{dE}\frac{dE}{dz} \approx 8\pi r_e^2 \frac{m_e c^2}{mc^2} N_0 \frac{Z}{A}\frac{\rho}{\gamma^3\beta^4}\left[\ln\frac{2\gamma^2\beta^2 m_e c^2}{I} - \gamma^2\right] \approx 8\pi r_e^2 \frac{m_e c^2}{m_\mu c^2} N_0 \frac{Z}{A}\frac{\rho}{\gamma^3\beta^4}(12-\gamma^2), \tag{20}$$

where the final approximation assumes $I \approx 15$ eV for the ionization potential of hydrogen. (This puts the dE/dz minimum at $\gamma = \sqrt{12}$, which is a bit low.)

Then, recalling (17), eq. (16) becomes

$$\begin{aligned} \frac{d(\Delta E)^2}{dz} &\approx 2\pi(r_e m_e c^2)^2 N_0 \frac{Z}{A}\rho\left[\frac{(\Delta E)^2}{m_e c^2 m_\mu c^2}\frac{4(12-\gamma^2)}{\gamma^3\beta^4} + (\gamma^2+1)\right] \\ &\approx \frac{\pi(m_e c^2)^2}{2\alpha(Z+1)\ln(287/\sqrt{Z})L_R}\left[\frac{48(\Delta E)^2}{m_e c^2}\frac{(1-\gamma^2/12)}{\gamma^2\beta^4 E} + (\gamma^2+1)\right]. \end{aligned} \tag{21}$$

This form reveals that the heating due to the variation in dE/dz with energy is proportional to $1/\beta^4$, which is perhaps the strongest argument against cooling at very low β.

For a hydrogen absorber, we can write (21) as

$$\frac{1}{(\Delta E)^2}\frac{d(\Delta E)^2}{dz} \approx \frac{466\ \text{MeV}(1-\gamma^2/12)}{\gamma^2\beta^4 E L_R}\left(1+\frac{1.1\ (\text{MeV})^2\gamma^3\beta^4(\gamma^2+1)}{(1-\gamma^2/12)(\Delta E)^2}\right). \tag{22}$$

For example, with $\gamma = 2$ (which is about the largest we can consider for transverse cooling) and $\Delta E \approx 10$ MeV, the first term in (22) is about twice the second, and

$$\frac{1}{(\Delta E)^2}\frac{d(\Delta E)^2}{dz} \approx \frac{1}{L_R}. \tag{23}$$

Recalling the example at the end of sec. 3.1.1, the transverse emittance ϵ_N was estimated to cool by a factor of 2 in $0.6L_R$. Equation (23) estimates that $(\Delta E)^2$ would grow by a factor of 1.8 over the same distance.

There is no value of γ for which the approximation (21) predicts longitudinal ionization cooling. However, our approximation underestimates the slope of dE/dz for $\gamma > 3$, due to our neglect of the density effect.

It is noteworthy that cooling (heating) scales as the radiation length with coefficients near unity (see eqs. (11) and (23)). Perhaps we could say loosely that ionization cooling is a manifestation of the very low energy tail of bremsstrahlung, and is in some sense a form of radiative cooling. This suggests we can find other aspects of ionization cooling in common with radiative cooling, as in the following section.

1.4 The Law of Damping Decrements

I read in sec. 8.2.3, p. 287 of [30] that Robinson [31] showed that for a process that damps the 6-d emittance of a bunch, the sum of the damping decrements of all 3 2-d subemittances is a constant. Robinson's paper does not give a general "proof", but an argument specific to radiative damping.

Here we follow [32] to consider the damping of the emittances, with the neglect of multiple scattering and straggling.

Thus, eq. (5) tells us that the transverse emittance $\epsilon_{\perp,N}$ has a damping distance $z_\perp$ given by

$$\frac{1}{z_\perp} = -\frac{1}{\beta^2 E}\frac{dE}{dz}. \tag{24}$$

When a particle traverses one damping distance in the absorber, it loses energy $E_\perp$ related by

$$\frac{1}{E_\perp} = -\frac{1}{z_\perp \frac{dE}{dz}} = \frac{1}{\beta^2 E}. \tag{25}$$

Similarly, eq. (14) for $(\Delta E)^2$ leads to a damping distance $z_{\Delta E}$ given by

$$\frac{1}{z_{\Delta E}} = -2\frac{d}{dE}\frac{dE}{dz}, \tag{26}$$

and the energy loss $E_{\Delta E}$ over this distance is

$$\frac{1}{E_{\Delta E}} = \frac{2\frac{d}{dE}\frac{dE}{dz}}{\frac{dE}{dz}} \approx -\frac{2}{\gamma^2\beta^2 E}\left(1 - \frac{\gamma^2}{12}\right), \tag{27}$$

where the approximation follows from (6-20).

We now consider the sum of the energy damping decrements of the 2-d emittances in x, y and ΔE. Noting that $E_x = E_y = E_\perp$, we have

$$\sum \frac{1}{E_i} = \frac{2}{E_\perp} + \frac{1}{E_{\Delta E}} = \frac{2}{\beta^2 E} + \frac{2\frac{d}{dE}\frac{dE}{dz}}{\frac{dE}{dz}} \approx \frac{2}{E}\left(1 + \frac{1}{12\beta^2}\right) \approx \frac{2}{E}, \tag{28}$$

where the first approximation is based on (27), and the second approximation is reasonable for β near 1.

It is implied in [32] that the final result of (28) is exact, but my derivation is not powerful enough to reveal this.

The impact of (28) for muon cooling is that strong transverse cooling implies strong longitudinal heating, even when neglecting multiple scattering and straggling!

1.5 An Ideal Cooling R&D Program

Ideally, the R&D program would study cooling with a muon beam that meets all the specifications at some point along the cooling channel at a muon collider or neutrino factory. Table 1 lists a present vision of the muon beam at the entrance to the cooling channel at a neutrino factory [8]. However, the only way to provide a muon beam that meets these specifications is to construct all elements of a neutrino factory up to the cooling channel. Further, at present there is no plausible diagnostic of the 6-dimensional emittance of such a beam – a situation that should be remedied by a separate R&D program.

1.6 The Single Particle Method

An affordable R&D program will have to compromise on the value of one or more parameters of the muon beam. A major cost savings can be obtained by use of a low-intensity muon beam. In this case, we lose the ability to study collective effects (space charge, wakefields, *etc.*). Optimistically, these effects are not large, particularly at a neutrino factory. However, this issue deserves additional theoretical study.

A useful definition of low intensity is that there be at most one charged particle within the apparatus at a time. Beam cooling studies under this condition have been called the single-particle method, whereby the phase-space parameters of individual muons are to be measured before and after a cooling apparatus, and the desired muon "bunch" reconstructed via software cuts. A modest-quality, low-intensity muon beam can be used for this method, and the muon parameters can be measured by techniques of high-energy physics experiments that emphasize precision measurement of a few particles at a time, rather than by beam monitors that typically measure only one coordinate of an intense beam. This strategy was adopted in cooling R&D proposals in 1995 [9] and 1998 [10, 11], but these proposals have not been acted upon.

Table 1: Phase-space parameters of the muon beam at the beginning of the cooling channel at a neutrino factory (after "minicooling").

Parameter	Value
Rep. rate	15 Hz
Muons/cycle	$\approx 10^{13}$
Bunches/cycle	≈ 50
Bunch frequency	≈ 200 MHz
P_0 (MeV/c)	185
E_0 (MeV)	213
γ	2.02
β	0.87
$\gamma\beta$	1.76
$\epsilon_{x,N} = \epsilon_{y,N}$ (π mm-mrad)	9,000
$\epsilon_x = \epsilon_y$ (π mm-mrad)	5,100
$\beta^\star$ (cm) [typical]	63
$\sigma_x = \sigma_y$ (mm)	57
$\sigma_{x'} = \sigma_{y'}$ (mrad)	90
σ_P/P	0.10
$\sigma_E/E = \beta^2\sigma_P/P$	0.076
σ_z (cm)	10
$\sigma_t = \sigma_z/\beta c$ (ps)	340

If the only compromise were to adopt the single-particle method, the ionization cooling R&D program would still very ambitious. Four prominent issues are the measurement of longitudinal emittance, the relatively slow rate of ionization cooling, x-rays from the rf cavities, and the muon beam.

1.7 Longitudinal Emittance Measurement

Ionization cooling only cools transverse space space (for muons of $\gamma \lesssim 3$), and "heats" the longitudinal phase space [13]. The latter can lead to loss of particles as the muon bunch grows larger than the "bucket" in longitudinal phase space. Hence, a significant goal of an ionization cooling R&D program is the characterization of longitudinal phase space growth.

The cooling apparatus includes rf cavities to replace the energy lost to ionization, and a bucket of longitudinal phase space extends over a limited range of phase of an rf cycle. In the single-particle method, the muons are distributed randomly with respect to rf phase, and the bucket can be properly reconstructed only from knowledge of the muon's timing within an rf cycle.

The rf frequencies under consideration range from 200 to 800 MHz, which leads to a requirement that the muon timing be measured to accuracy for 10-40 psec (higher accuracy for higher frequency). This demanding requirement adds considerable complexity to the

emittance instrumentation in the single-particle approach.

1.8 The Slow Rate of Cooling

A simple analytic model of ionization cooling (Appendix A, which ignores the effect of the solenoid field) predicts that the 2-d transverse emittance cools at the rate

$$\frac{1}{\epsilon_\perp}\frac{d\epsilon_\perp}{dz} \approx -\frac{1.8}{L_R}\left(1-\frac{\epsilon_{\perp,\mathrm{min}}}{\epsilon_\perp}\right), \tag{29}$$

for muons of momentum 185 MeV/c, where L_R is the radiation length of the absorber in which the ionization occurs.

A significant demonstration of transverse cooling would involve a 50% reduction in $\epsilon_\perp$, say from $4\epsilon_{\perp,\mathrm{min}}$ to $2\epsilon_{\perp,\mathrm{min}}$. If the absorber is liquid hydrogen ($L_R = 866$ cm), this requires $0.6L_R \approx 500$ cm. Meanwhile, the muons lose about 0.3 MeV/cm in the liquid hydrogen, for a total energy loss of 150 MeV.

As in an eventual cooling channel, the lost energy could be replenished by acceleration in rf cavities, whose total length would be 20 m if the effective accelerating gradient were 7.5 MeV/m (for 200 MHz cavities with peak fields on axis of 15 MeV/m). The rf cavities occupy about half the length of the cooling apparatus, consisting of alternating regions of absorption and acceleration. Thus, the length of an apparatus to cool by 50% is about 40 m. Throughout this length, the muons are confined in a channel of superconducting solenoids.

1.9 X-Rays

Rf cavities are in general prolific sources of x-rays, due to bremsstrahlung of thermal- and field-emission electrons that are accelerated across the cavity. The effect of these x-rays on the single-particle instrumentation before and after the cooling apparatus could well be such that present visions of gas tracking and Čerenkov timing devices are untenable. This issue is currently under study [14].

1.10 The Muon Beam

While only a "modest" muon beam is needed for the single-particle method, such beams are in short supply. Decommissioned muon beams still exist are BNL and LANL, but the only operating, low-energy muon beams in the western hemisphere are at TRIUMF.

1.11 A Phased Cooling R&D Program

The issues sketched in secs. 1.3-6 have led to the formulation of a phased cooling R&D program [15, 16] with technical development of components of the cooling apparatus proceeding in parallel with a sequence of beam tests, culminating in a demonstration of transverse cooling by about 50% in an apparatus of about 20 periods of absorbers and rf cavities inside a suitable modulated solenoid transport line. Study of longitudinal/transverse emittance exchange is a desirable part of the R&D program, but likely would occur in a later phase.

This note emphasizes a first step in the beam tests, motivated by the opportunity to make an important physics demonstration of transverse emittance cooling as quickly as possible using an existing beam and solenoid magnet. The compromise is that this first study would not test any of the apparatus of a more sophisticated cooling channel, but would demonstrate only the effect of a simple absorber in a uniform solenoid field, such as foreseen in the "minicooling" stage of a neutrino factory source [8, 6, 17]. However, it will demonstrate the important coupling of transverse emittance and canonical angular momentum of beams inside a solenoid, which greatly adds to the complexity of the design of a practical ionization cooling channel **(need ref and/or pointer)**.

A possible sequence of beam tests, all using the single particle method, in the cooling R&D program could then be:

1. Test of ionization cooling by a single absorber in a uniform solenoid field without rf acceleration. Diagnostics would reside inside the same solenoid as the absorber. A 9% reduction in normalized transverse emittance of 10,000 π mm-mrad could be demonstrated.

2. Test of angular momentum control in a "single-flip" solenoid.

3. Test of a single period of a cooling channel that contains an absorber, an rf cavity and a modulated solenoid magnet. The frequency of the rf cavity could be about 200 MHz to study normalized emittance of 10,000 π mm-mrad as at the entrance to the cooling channel of a neutrino factory source, or about 800 MHz to study normalized emittance of 1,500 π mm-mrad as in a late stage of cooling for a muon collider source. Diagnostics would reside inside separate solenoid magnets. For precision measurement of longitudinal emittance, the diagnostic magnets will likely be bent solenoids. Again, a 5% reduction in normalized transverse emittance would be demonstrated.

4. Test of 10 periods of a cooling channel that contain absorbers, rf cavities and a modulated solenoid magnet lattice. A 50% reduction in normalized transverse emittance would be demonstrated.

5. Test of longitudinal/transverse emittance exchange by a technology to be determined.

Tests of ionization cooling in a high-intensity, bunched muon beam require construction of such a beam. This may require construction of a new muon beam, perhaps using a small muon ring [18], but might also be accomplished by use of the MECO muon channel [19] if operated with a bunched proton beam.

2 A Simple First Demonstration of Ionization Cooling

Here, we propose a simple first step in beam tests of ionization cooling that is on the critical path towards a more complete cooling demonstration, and could proceed rapidly while the design of the latter matures.

The scope of the proposed initial cooling study is:

1. Use the single-particle method.

2. Study ionization cooling without rf acceleration. The cooling apparatus is simply an absorber in this case. This corresponds to the minicooling stage of a neutrino factory source [8, 17].

3. Surround the absorber with low-pressure gas tracking and Čerenkov particle ID.

4. Place the tracking devices and the absorber inside a single existing solenoid, such as the TRIUMF E614 magnet [20], or the LASS magnet [21]. A sketch of this is given in Fig. 1. This permits investigation of the theoretical minimum of emittance cooling that depends on the strength of the beam confining apparatus. A resonable study of longitudinal emittance growth due to straggling will be possible as well.

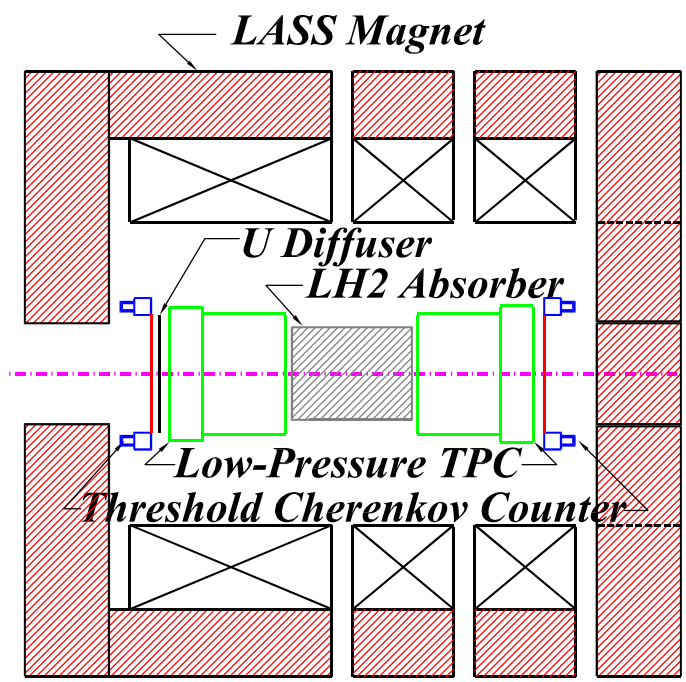

Figure 1: Configuration of a simple cooling experiment inside the LASS magnet.

5. Use the existing D2 π/μ channel at BNL (or a new beamline to be built at FNAL).

6. In the option to perform the first step at BNL, we would accept the existing experimental area at the end of the D2 line essentially as is. Figure 2 sketches a possible layout.

This first step would accomplish the following goals:

1. Demonstrate the single-particle method. This method is little known to the accelerator community, so it will be very useful to have an early mechanism to demonstrate its validity. The heart of this method is software, which must be developed almost as fully to reconstruct 4-d phase space as the eventual 6-d phase space.

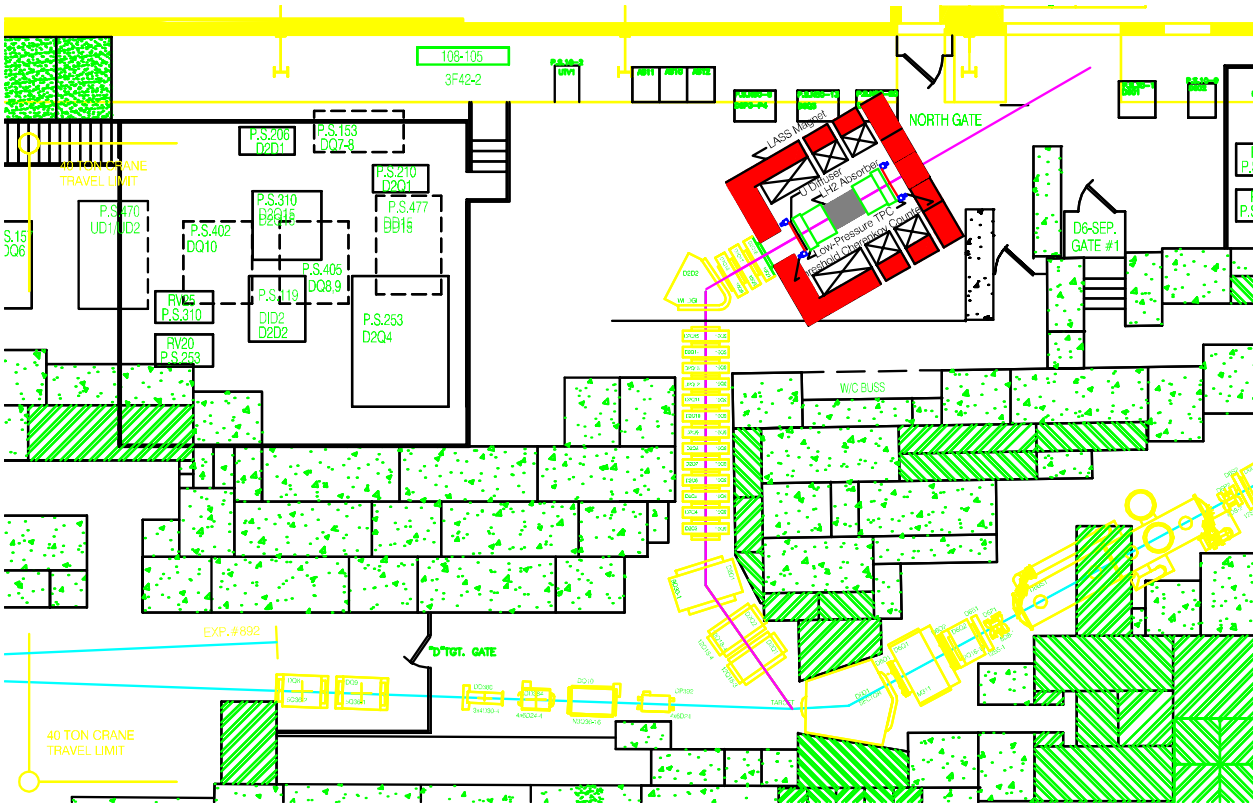

Figure 2: Possible layout of the simple cooling experiment in the D2 line at BNL.

2. Perform precision measurement of multiple scattering and straggling for low-energy muons in LH_2 and other absorbers in a magnetic field.

3. Demonstrate transverse cooling and longitudinal emittance growth of a software-selected "bunch" of muons.

4. Validate the analytic and numerical studies of ionization cooling.

5. Develop instrumentation to measure transverse emittance.

6. Recommission the D2 line, which is a necessary first step towards possible transportation and use of that line to FNAL.

2.1 The Beamline

As indicated in Table 1, we would like to study cooling of a muon bunch of initial normalized transverse emittance $\epsilon_{\perp,N} \approx 10,000\ \pi$ mm-mrad, and central momentum near 180 MeV/c ($\beta = 0.87$).

The existing second dipole magnet, D2D2, in the D2 line is believed to bend a maximum of 124 MeV/c by 90°. The layout of the D2 area makes it more appropriate to bend the muons by only 60°, as shown in Fig. 2, to avoid interference with existing water pipes on

the east wall of the cave (bottom of figure), and to permit access to the detectors from the downstream end of the magnet (by removing the steel endcap). Further, the D2D2 magnet is actually a 60° wedge magnet, which is more naturally operated with a 60° than a 90° bend For a 60° bend, the maximum momentum would be 184 MeV/c.

The BNL D2 line has been run only rarely, but it has been confirmed that under conditions similar to those proposed the muon yield is about 10^{-6} per proton on target. The rates in the proposed experiment will be limited by the data acquisition system rather than by the beam flux.

2.1.1 Transverse Emittance

As indicated in Table 1, we would like to study cooling of a muon bunch of initial normalized transverse emittance $\epsilon_{\perp,N} \approx 10,000\ \pi$ mm-mrad (geometric emittance $\epsilon_\perp \approx 6,000\ \pi$ mm-mrad), and central momentum near 180 MeV/c ($\beta = 0.87$).

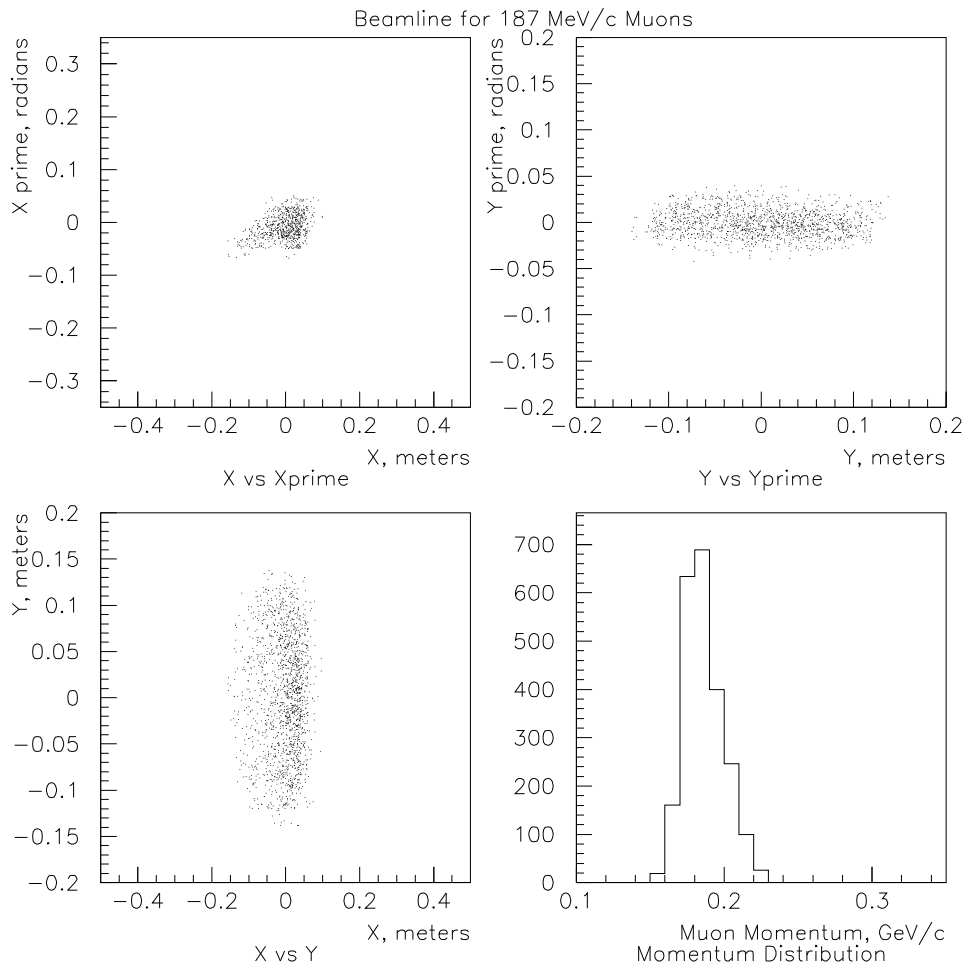

Figure 3: Simulation of a 187 MeV/c muon beam produced in the D2 line using pions of 300 MeV/c (using an upgraded version of magnet D2D2).

A simulation of a 187 MeV/c muon beam at the end of the D2 line [10], shown in Fig. 3, indicates that the rms transverse size of the beam is about 5 cm and the rms transverse angle is about 20 mrad. That is, the geometric transverse emittance is $\epsilon_\perp \approx 1,000\ \pi$ mm-mrad, which is only about 15% of that desired for the study. The spatial extent of the beam is about right, but the angular spread is much smaller than desired. (This is a general feature of quadrupole beam transport, in contrast to solenoid transport which can accommodate much larger angles.)

To increase the rms angular spread to 120 mrad, a 2-radiation-length-thick diffuser should be placed close to the effective upstream edge of the solenoid field (so as to increase the muon angles but not the beam size); then, $\theta_{\rm rms} = 14\sqrt{X}/P\beta = 14{\cdot}\sqrt{2}/184{\cdot}0.87 = 0.12$. To degrade the beam energy as little as possible, the diffuser should be a high-Z material, preferably uranium. In that case the energy loss is about 7 MeV per radiation length, for a total loss of 14 MeV in the diffuser. The central beam momentum after the diffuser would then be 168 MeV/c, which is the proposed central momentum for the simple cooling study. Parameters of the D2 beamline are summarized in Table 2.

2.1.2 Matching and Angular Momentum

As a muon exits the quadrupole channel and enters the solenoid field, the axial (z) component of its angular momentum is conserved:

$$L_z = r\Pi_\phi = r\left(P_\phi + \frac{eA_\phi}{c}\right) \approx rP_\phi + \frac{er^2B_z}{2c}, \tag{30}$$

where

$$\Pi = \mathbf{P} + \frac{e\mathbf{A}}{c} \tag{31}$$

is the canonical momentum. For a solenoid magnet driven by azimuthal currents, the only nonzero component of the vector potential is

$$A_\phi(r,z) = \frac{1}{r}\int_0^r r'B_z(r',z)dr' \approx \frac{rB_z}{2}. \tag{32}$$

Muons from the quadrupole channel would in general have zero azimuthal momentum P_ϕ, and hence $L_z = 0$. On entering the solenoid magnet, however, they experience an azimuthal kick, resulting in

$$P_\phi\ [\text{MeV}/c] = -\frac{erB_0}{2c} = -150\ r\ [\text{m}]B_0\ [\text{T}]. \tag{33}$$

according to eq. (30), where B_0 is the value of the axial magnetic field inside the solenoid.[2] We will have muons at radii up to 0.2 m entering the solenoid, so that P_ϕ will be as large as 75 MeV/c for $B_0 = 2.5$ T. The corresponding angle of the muon to the beam axis will be as large as 400 mrad, which is larger than the intrinsic angular spread of the beam even after the diffuser.

The strong correlation between r and P_ϕ means that a "naive" analysis of x and y transverse emittances would be misleading. The appropriate analysis is of the normalized

[2]This also follows from $\nabla\cdot\mathbf{B} = 0$, which implies that $B_r = -(r/2)\partial B_z/\partial z$, so that $P_\phi = \int F_\phi dt = \int ev_zB_rdt/c = -(er/2c)\int(\partial B_z/\partial z)dz = -erB_0/2c$.

Table 2: Parameters of the proposed muon beam in the BNL D2 line.

Parameter	Value
Before diffuser:	
P_0 (MeV/c)	184
E_0 (MeV)	212
$\sigma_x = \sigma_y$ (mm)	50
$\sigma_{x'} = \sigma_{y'}$ (mrad)	20
After diffuser:	
P_0 (MeV/c)	168
E_0 (MeV)	198
γ	1.89
β	0.85
$\gamma\beta$	1.60
$\epsilon_{x,N} = \epsilon_{y,N}$ (π mm-mrad)	10,000
$\epsilon_x = \epsilon_y$ (π mm-mrad)	6,250
$\beta^\star$ (cm) at 2.5 T	45
$\epsilon_{x,N\mathrm{min}} = \epsilon_{y,N,\mathrm{min}}$ (π mm-mrad)	1,500
$\sigma_x = \sigma_y$ (mm)	53
$\sigma_{x'} = \sigma_{y'}$ (mrad)	120
$\sigma_{\Pi_x} = \sigma_{\Pi_y}$ (MeV/c)	20
σ_P/P	0.10
$\sigma_E/E = \beta^2\sigma_P/P$	0.076
After 50 cm LH_2 absorber:	
P_0 (MeV/c)	150
E_0 (MeV)	183
$\gamma\beta$	1.43
$\epsilon_{x,N} = \epsilon_{y,N}$ (π mm-mrad)	9,100
$\epsilon_x = \epsilon_y$ (π mm-mrad)	6,370

transverse emittance using canonical coordinates, x, y, $\Pi_x = P_x - e\sin\phi A_\phi/c \approx P_x - eyB_z/2c$ and $\Pi_y \approx P_y + exB_z/2c$. The vector potential A_ϕ can be well determined from eq. (32) using a field map of the magnet. The detector must measure the transverse coordinates (x, y) and transverse momentum (P_x, P_y) as input to the calculation of the normalized transverse emittance defined by

$$m^2c^2\epsilon_{x,N}^2 = \left\langle x^2 \right\rangle \left\langle \Pi_x^2 \right\rangle - \left\langle x\Pi_x \right\rangle^2 , \tag{34}$$

and similarly for $\epsilon_{y,N}$.

2.2 Performance Goals

2.2.1 Multiple Scattering

Tollestrup [22, 23, 24] has discussed the limitations of the Moliere scattering theory for light elements, and Lebrun [25] has noted possible limitations of simulations of multiple scattering in the presence of a strong magnetic field.

One issue is the accuracy of our simulations of large-angle scattering in the absorber, which scatters can be associated with particle loss. Figure 4 from [23] illustrates various models of the multiple scattering distribution for 186 MeV/c muons in 32 cm of liquid hydrogen. The nongaussian tail at angles above 60 mrad indicates the regime where single scatters dominate, and where the greatest model uncertainty lies.

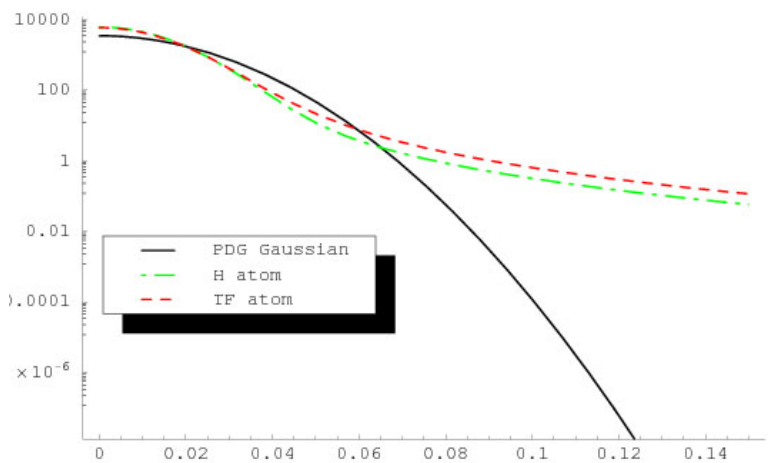

Figure 4: The distribution of multiple scattering angles for 186 MeV/c traversing 32 cm of liquid hydrogen according to three models. From [23].

A detector resolution of order 1 mrad will be adequate to characterize the single scattering tail. Since the tail includes less than 10^{-3} of all scatters, fairly large event samples will be required. For example, some 10^6 events would determine the magnitude of the tail to about 10%, while 10^8 events would be needed for a 1% determination, *etc.*

The issue of scatter in a magnetic field is more important for small scattering angles, where the magnetic deflection of the muon's trajectory between scatters can be larger than the scattering angle. As illustrated in Fig. 5, this effect narrows the scattering angle distribution slightly, and the distribution of transverse displacements more significantly. While this effect is well understood in principle, it will be useful to collect data that can validate our simulations. For this detector resolutions of order 1 mm in transverse coordinates, and of order 1 mrad in angle are desirable. *[These are a first estimate, which should be quantified by further simulation.]*

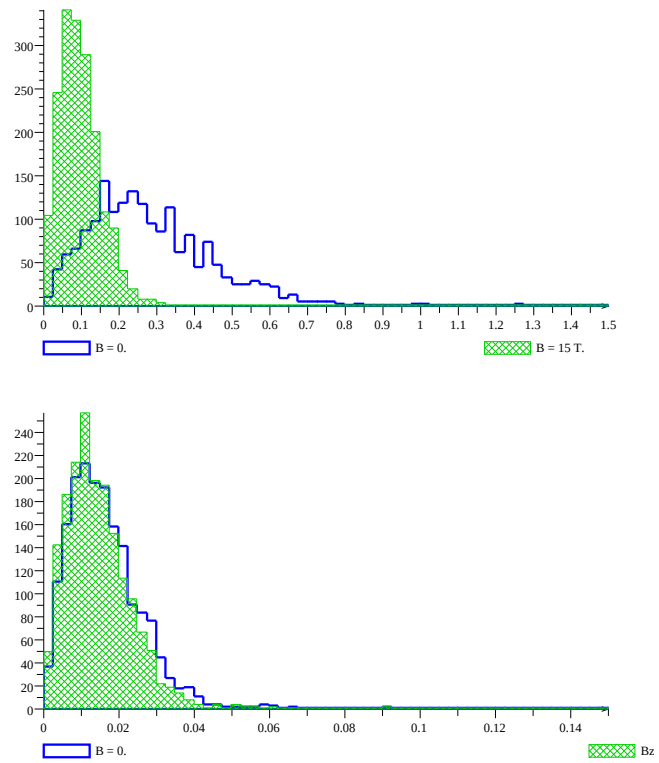

Figure 5: The distributions of transverse displacement (top) and scattering angle (bottom) for 186 MeV/c muons traversing 32 cm of liquid hydrogen, both in zero magnetic field and in a solenoidal field of 15 T. From [25].

2.2.2 Transverse Emittance

When the bunch is confined in a channel, the transverse emittance can be cooled by a liquid hydrogen absorber only to

$$\epsilon_{\perp,N,\min} = \frac{0.0038\beta\beta_\perp^\star}{1-\beta^2/12}, \tag{35}$$

due to "heating" by multiple Coulomb scattering (see Appendix A).

The betatron function for a solenoid of axial field B_z depends on the particle momentum according to (see sec. 5 of [12])

$$\beta_\perp^\star\ [\mathrm{m}] = \frac{2cP_z}{eB_z} = \frac{P_z\ [\mathrm{MeV}/c]}{150B_z\ [\mathrm{T}]}. \tag{36}$$

For example, with $P_z = 168$ MeV/c ($\beta = 0.85$) and $B_z = 2.5$ T, we have $\beta_\perp^\star = 0.45$ m, and the corresponding minimum transverse emittance in a liquid hydrogen cooling channel follows from eq. (35) as $\epsilon_{\perp,N,\min} = 0.0015\ \pi$ m-rad $= 1{,}500\ \pi$ mm-mrad.

The rate of cooling in liquid hydrogen then follows from eq. (29) as

$$\frac{1}{\epsilon_\perp}\frac{d\epsilon_\perp}{dz} \approx \frac{0.18}{[\mathrm{m}]}. \tag{37}$$

A liquid hydrogen absorber of length 0.5 m would lead to cooling of the normalized transverse emittance by about 9%. To observe such cooling, the apparatus should measure the transverse emittance to, say 1%.

As discussed in Appendix B, this can be achieved via the single-particle technique with about 10^4 muons provided the detector resolution obeys

$$\sigma_{D,i} < \sqrt{2.5\frac{\delta_{\epsilon_\perp}}{\epsilon_\perp}}\sigma_i = 0.16\sigma_i, \tag{38}$$

for $i = x$, y, P_x, and P_y. For the proposed experiment, Table 2 lists σ_x as 53 mm and σ_{π_x} as 20 MeV/c. Hence we desire detector resolution of $\sigma_{D,x} < 8$ mm and $\sigma_{D,P_x} < 3$ MeV/c. This performance is readily achieved, so we also consider some more demanding requirements.

Geometric Transverse Emittance

An interesting "paradox" is that while the normalized emittance is decreasing, the geometric emittance is actually increasing. This occurs because the muons lose energy in the absorber faster than the bunch loses emittance, so that the geometric emittance $\epsilon_\perp$ rises, according to the relation

$$\epsilon_\perp = \frac{\epsilon_{\perp,N}}{\gamma\beta}, \tag{39}$$

where γ and β are the average Lorentz factors of the bunch. Of course, when the lost energy is restored by rf acceleration, the geometric emittance falls as well (while the normalized emittance in unchanged by the rf).

For the present example, the muons lose about 15 MeV energy ($\Delta P/P \approx 11\%$) in the 50-cm-thick liquid hydrogen absorber, and the geometric transverse emittance grows by 1.9%. For the experiment to provide a good demonstration of the effect of an absorber on transverse emittance, we should make an explicit measurement of the growth of the geometric emittance. To observe a 2% growth, the instrumentation should be able to determine the geometric transverse emittance to, say, 0.2%. Then, according to eq. (38), the detector resolution should be $\sigma_{D,i} < 0.07\sigma_i$.

For a muon bunch centered at 168 MeV/c momentum with normalized transverse emittance of 10,000 π mm-mrad, the geometric transverse emittance is

$$\epsilon_\perp = \frac{\epsilon_{\perp,N}}{\gamma\beta} = \frac{10,000}{1.60} = 6,250\ \pi \text{ mm-mrad}, \tag{40}$$

so in a 2.5-T solenoid, the $\beta_\perp^\star$ is 45 cm, and the corresponding rms widths are

$$\sigma_x = \sqrt{\epsilon_\perp\beta_\perp^\star} = 53 \text{ mm}, \qquad \text{and} \qquad \sigma_{x'} = \sqrt{\frac{\epsilon_\perp}{\beta_\perp^\star}} = 120 \text{ mrad}. \tag{41}$$

We therefore need detector resolutions of $\sigma_{D,x} \leq 3.5$ mm and $\sigma_{D,x'} \leq 8$ mrad.

In sec. 4.9 of [11] we argued that a low-pressure time projection chamber suitable for diagnosing both longitudinal and transverse emittance in a single-particle experiment would have resolution $\sigma_{D,x} \approx 200$ μm and $\sigma_{D,x'} < 1$ mrad. This performance is considerably better than the minimum requirement for a measurement of geometric transverse emittance cooling in the present experiment, and would permit a fairly good momentum measurement

of large angle muons as well. Since normalized emittance cooling should be observed when the geometric emittance is divided by the $\gamma\beta$ of the bunch, it will be useful if the apparatus can measure the value of this quantity before and after the absorber. The accuracy should be about 1%, in case of an expected 11% reduction in momentum.

A single TPC in an axial magnetic field can measure a muon's total momentum to accuracy given by $\sigma_{D,P}/P = \sigma_{D,\theta}/\theta$, which deteriorates for small-angle muons. A detector resolution of $\sigma_{D,x'} \approx 1$ mrad yields $\sigma_{D,P}/P \approx 0.01$ for muons with angles greater than 100 mrad. Because of the kick (33) of $P_\phi = 375$ MeV$/c \cdot r$ [m] on entering the 2.5-T solenoid, muons at radii larger than 4.5 cm take on angles of at least 100 mrad. Further, for the large emittance study the rms angle is $\sigma_{x'} \approx 120$ mrad, not counting the P_ϕ kick, so a significant momentum measurement can be made for muons with either a large angle or a large radius. This should permit a good confirmation of the expected 11% momentum loss in the absorber.

A precise momentum measurement of small angle muons is not readily accomplished with a solenoid spectrometer. Rather, transverse dipole magnets would need to be added, either in the form of bent solenoids as proposed in [10, 11], or with the addition of H-type dipole magnets outside of the solenoid magnet as sketched in Appendix C.

2.2.3 Longitudinal Emittance

While the normalized transverse emittance is cooled by ionization, the longitudinal emittance is increased due to energy straggling in the absorber. Indeed, eq. (23) of Appendix A estimates the leading effect as a growth in the energy spread of the muon bunch according to

$$\frac{1}{(\Delta E)^2}\frac{d(\Delta E)^2}{dz} \approx \frac{1}{L_R}. \tag{42}$$

It is noteworthy that in the absence of rf acceleration, there is no need to know the timing of the muons to study longitudinal emittance growth.

For a 0.5-m-long liquid hydrogen absorber, eq. (42) predicts that $\delta(\Delta E)^2 = 0.06(\Delta E)^2$, and hence, $\delta(\Delta E)/\Delta E \approx 3\%$. From Table 2, we see that the rms ΔE of the muon bunch is about 15 MeV, so the expected blowup of this is about 0.5 MeV. We would therefore like to measure ΔE to about 0.1 MeV, which requires $\delta_{\sigma_P}/\sigma_P = \delta_{\Delta E}/[\beta^2 \Delta E] = 0.1/[(.85)^2 \cdot 15] = 0.01$.

According to the discussion in sec. 4.2.3, of Appendix B, to measure such an effect with the single-particle method we would need momentum $\sigma_{D,P} \approx \sqrt{0.01/0.2}\sigma_P = 0.22\sigma_P \approx 0.22 \cdot 17 \approx 4$ MeV$/c$. The corresponding momentum resolution is $\sigma_{D,P}/P \approx 0.02$ From the discussion at the end of the preceding section, a measurement of this accuracy is possible for muons of angles $\gtrsim 50$ mrad or radius greater than 2 cm in the proposed solenoid spectrometer. Hence, it should be possible to do a partial study of longitudinal emittance growth in the proposed simple experiment.

2.3 Instrumentation

2.3.1 Time Projection Chambers

We propose the use of low-pressure TPC's to track the particle trajectories before and after the absorber. Although the momentum measurement is not emphasized in the simple cooling demonstration, there is little technical cost in using a chamber of the same design as appropriate for an experiment that includes momentum measurement. See, for example, [26]. The use of a 2.5-T magnetic field then leads to chamber parameters very similar to those for final-stage cooling studies [11]: 50 cm tracking length, and 33 clusters/m ionization density (corresponding to operation at about 0.01 atmosphere pressure).

In sec. 2.6.2 of [11] we argued that the fiducial radius of the solenoid field (= radius of absorber and detector) should be about $3\sigma_{R,\max} \approx 6\sigma_x$. In the present case, we study σ_x up to 5 cm, so the chamber radius is 30 cm (compared to only 10 cm for the final-stage cooling case discussed in [11]). If we keep the channel count at 1250 per TPC, the pad width is now 15 mm. Laboratory studies need to be performed to verify that the nominal spatial resolution of $\sigma_{D,x} = 200$ μm can be achieved for such large pads. If not, the channel count will have to increase.

2.3.2 Particle ID

For a central muon momenta of 150 MeV/c, $\pi\mu/e$ particle identification can readily be accomplished by use of threshold Čerenkov counters with a water radiator (index = 1.33), while for 168 MeV/c it would be better to use a C_6F_{14} radiator, as shown in Fig. 6 [27]. The Čerenkov photons could be detected via an array of fine-mesh photomultiplier tubes next to the radiator, as sketched in Fig. 1. The liquid radiators would be contained in "pillboxes" with mirror surfaces. Broadband mirrors have only 98% reflectivity at best for wavelengths below 400 nm, as shown in Fig. 7, so the radiators should be several cm thick.

2.3.3 Solenoid Magnet

We propose to use the LASS solenoid magnet [21] because it is available, has large enough dimensions, and can operate at fields up to 2.5 T. We would use the magnet in the configuration utilized by the MEGA experiment at LANL in which one of the original coils is omitted, and the original large upstream aperture is filled with an iron plug. This is the configuration shown in Figs. 1 and 2.

The modular construction of the LASS magnet results in a somewhat nonuniform axial field, which is less than ideal for use with time projection chambers. As shown in Fig. 8, the axial field of the LASS magnet varies by about 1.5% over 50 cm in z for radii less than 30 cm, due to the discrete coil packages. In a TPC, the ionization electrons follow magnetic field lines as they drift to the cathode. To reconstruct the source of the ionization, one must know how much the field lines have bent. Since the magnetic flux is Br^2, this quantity is constant along field lines. Hence, along a field line,

$$\frac{dr}{r} = \frac{1}{2}\frac{dB}{B}. \tag{43}$$

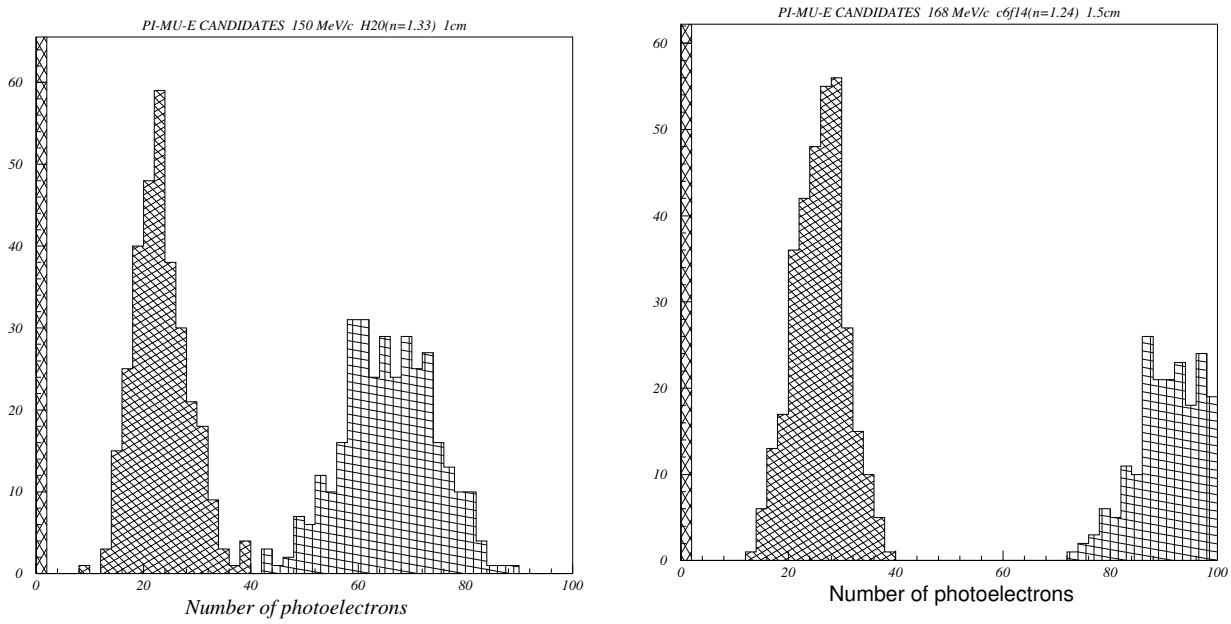

Figure 6: Simulated spectrum of number of photoelectrons detected from a 150 MeV/c π's, μ's and e's in a 1-cm-thick water radiator (left), and from 168 MeV/c π's, μ's and e's in a 1.5-cm-thick C_6F_{14} radiator (right). From [27].

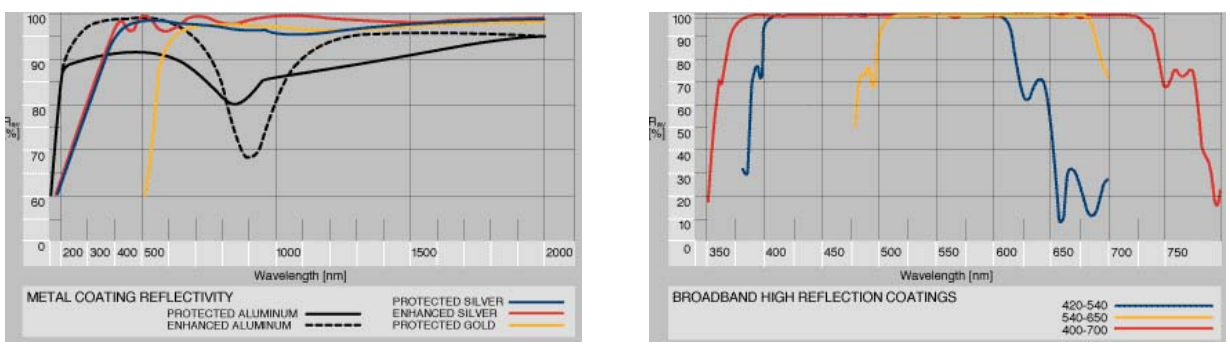

Figure 7: Reflectivities of commercial mirror coatings. From OptoSigma Co.

Over the 50 cm length of a TPC, and at the maximum radius of 30 cm, the radial coordinate of a field line could vary as much as $\Delta r = r\Delta B/2B \approx 30$ cm $\cdot$ 0.015/2 = 2.25 mm. To reconstruct the location of the ionization to 200 μm, the size of the change in the field strength would need to be known to about 1/10 of the change, *i.e.*, to about 0.0015. Since this is the typical accuracy of a magnetic field map, we should be able to use the LASS magnet as is, after making a map.

2.4 Run Strategy

Initial runs would be at 2.5 T in the solenoid magnet, with a diffuser but without any absorber. This would permit the beam emittance to be measured twice, in the first and

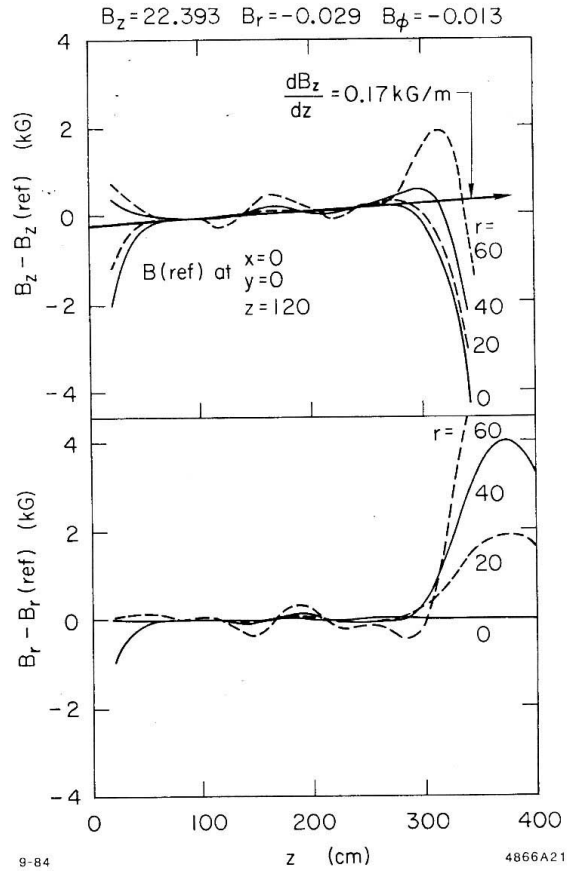

Figure 8: Data from a map of the LASS solenoid magnet [21].

second TPC's, to validate the accuracy of the measurement. Runs would then be made with both liquid hydrogen and lithium hydride absorbers. Software cuts will permit selection of initial emittances smaller than the maximum permitted by apertures; for initial emittances $\leq \epsilon_{\perp,N,\mathrm{min}}$ no cooling should be observed.

While runs of only 10^4 muons should be sufficient for studies of the full emittance within the solenoid acceptance, the study of emittance near the cooling minimum will involve cutting away all but about $(\epsilon_{\perp,\mathrm{min}}/\epsilon_{\perp,\mathrm{max}})^2 \approx 1/40$ of the muons. Such runs would therefore require roughly 10^6 muons.

If the diffuser is removed, the emittance of the beam from the muon channel is much closer to the cooling minimum, and the runs could be shorter. Comparisons would be made between software "bunches" of muon of the same emittance obtained with and without the diffuser.

3 Appendix B: Measurement Accuracy

This section is adapted from sec. 2 of [11].

3.1 Combined Accuracy

Ignoring correlations, the transverse emittance of the muon bunch can be written as $\epsilon_\perp \propto \sigma_x \sigma_{q_x} = \sigma_y \sigma_{q_y}$, where $q_x = P_x$ in case of normalized emittance, $q_x = x'$ for geometric emittance, and σ_i^2 is the variance (second moment) of the distribution of muons on phase-space coordinate i. We call σ_i the rms width. The uncertainty in σ_i is labelled δ_{σ_i}. Then, the uncertainty in the transverse emittance is

$$\frac{\delta_{\epsilon_\perp}}{\epsilon_\perp} = \sqrt{\left(\frac{\delta_{\sigma_x}}{\sigma_x}\right)^2 + \left(\frac{\delta_{\sigma_{x'}}}{\sigma_{x'}}\right)^2}. \tag{44}$$

For example, in sec. 2.2.1 we indicated that the desired accuracy of the measurement of geometric transverse emittance is that $\delta_{\epsilon_\perp}/\epsilon_\perp = 0.002$, so if the relative uncertainties in σ_x and $\sigma_{x'}$ are equal, they each must be 0.0014.

3.2 Effect of Detector Resolution

In the Gaussian approximation, the observed rms width σ_O of a projected phase-space distribution is sum in quadrature of the 'true' rms width σ_i and the rms width σ_D of the detector resolution:

$$\sigma_O^2 = \sigma_i^2 + \sigma_D^2. \tag{45}$$

We suppose that σ_D is known to an accuracy δ_{σ_D}. Then, we extract the desired rms width σ_i according to

$$\sigma_i^2 = \sigma_O^2 - \sigma_D^2. \tag{46}$$

We now wish to characterize the uncertainty δ_{σ_i}. From eq. (46) we find

$$\delta_{\sigma_i^2}^2 = \delta_{\sigma_O^2}^2 + \delta_{\sigma_D^2}^2. \tag{47}$$

Next, the uncertainty in the observed variance σ_O^2 after a set of N measurements is[3]

$$\delta_{\sigma_O^2} = \sqrt{\frac{2}{N}}\sigma_O^2 = \sqrt{\frac{2}{N}}\left(\sigma_i^2 + \sigma_D^2\right). \tag{48}$$

Then, noting that $\delta_{\sigma^2} = 2\sigma\delta_\sigma$ we find the key result:

$$\left(\frac{\delta_{\sigma_i}}{\sigma_i}\right)^2 = \frac{1}{2N}\left(1 + \frac{\sigma_D^2}{\sigma_i^2}\right)^2 + \left(\frac{\sigma_D}{\sigma_i}\right)^4 \left(\frac{\delta_{\sigma_D}}{\sigma_D}\right)^2. \tag{49}$$

3.2.1 Perfectly Known Resolution

In the limit that the detector resolution is completely understood we have $\delta_{\sigma_D} = 0$, and the relative uncertainty in the rms width σ_i is

$$\frac{\delta_{\sigma_i}}{\sigma_i} = \sqrt{\frac{1}{2N}}\left(1 + \frac{\sigma_D^2}{\sigma_i^2}\right). \tag{50}$$

[3]See, for example, sec. 28.2 of the chapter on *Statistics* of the *Review of Particle Properties* (1996).

If the detector resolution σ_D is larger than the rms width σ_i we wish to measure, the number of events required to achieve a specified accuracy, $\delta_{\sigma_i}/\sigma_i$ varies as the fourth power of the ratio σ_D/σ_i.

Thus, there is a severe statistical penalty unless

$$\sigma_D < \sigma_i. \tag{51}$$

However, once relation (51) is satisfied,

$$\frac{\delta_{\sigma_i}}{\sigma_i} \approx \sqrt{\frac{1}{2N}}. \tag{52}$$

In this case, only 1,250 single-particle measurements would be required to reach the desired relative uncertainty in σ_i of 0.02.

For the simple cooling experiment considered here, a large fraction of all muons passing through the apparatus will survive the software bunch cuts, and it is likely that a typical run would require measurement of $\lesssim 10^4$ muons.

3.2.2 Large-N Limit

In the other limit that counting statistics, but not detector resolution, can be neglected, we have

$$\frac{\delta_{\sigma_i}}{\sigma_i} = \left(\frac{\sigma_D}{\sigma_i}\right)^2 \frac{\delta_{\sigma_D}}{\sigma_D}. \tag{53}$$

Good results can only be obtained if σ_D/σ_i is less than one, unless the detector resolution is extraordinarily well understood. However, if σ_D/σ_i is much less than one, very good results are possible.

3.2.3 Maximum Acceptable Detector Resolution

To achieve the goal of measurement accuracy $\delta_{\sigma_i}/\sigma_i = 0.7\delta_\epsilon/\epsilon$ we require that the effect of detector resolution be no more than half in quadrature, *i.e.*, less than $0.5\delta_\epsilon/\epsilon$ as the number of measurements grows large.

Suppose that the uncertainty in the detector resolution function will be no more than 20%:

$$\frac{\delta_{\sigma_D}}{\sigma_D} < 0.2. \tag{54}$$

Then eq. (53) tells us that the detector resolution must obey

$$\sigma_{D,i} < \sqrt{2.5\frac{\delta_\epsilon}{\epsilon}}\sigma_i. \tag{55}$$

4 Appendix C: The 1995 Letter of Intent

The present proposal is similar in spirit to a Letter of Intent presented to the BNL AGS in 1995 [9]. The layout of that proposal is sketched in Fig. 9. The emphasis was on cooling of

emittances of order 100-1000 π mm-mrad, leading to the proposed use of a 7-T solenoid with a lithium absorber. The diagnostics were to be a pair of spectrometers based on large H-magnets surrounded by planar drift chambers. Although rather large detectors are required to study muons of angles up to, say, 300 mrad, this configuration permits good momentum measurement of all muons. However, the efficiency is low for transport of such large angle muons into the absorber in the solenoid, in contrast to a configuration with detectors and absorber in a single solenoid as proposed here.

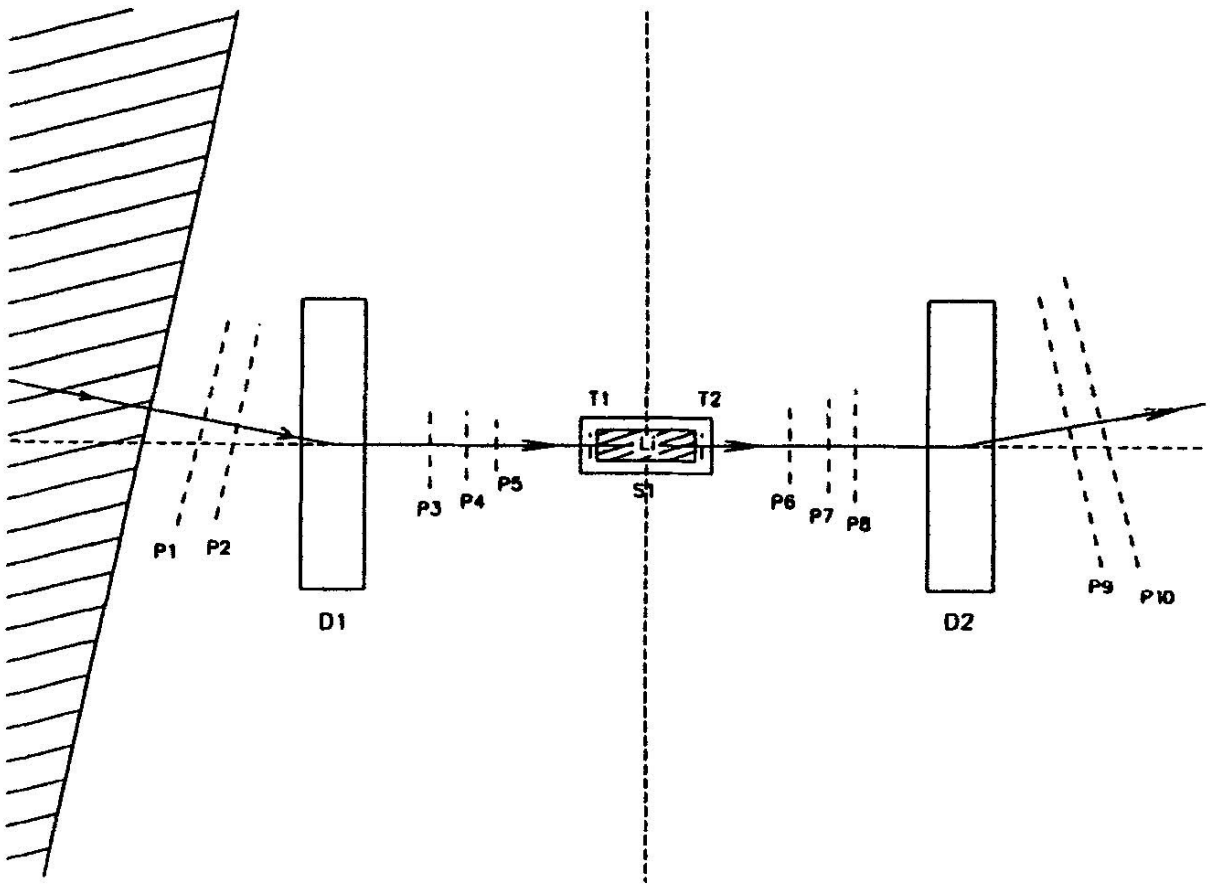

Figure 9: Layout of a cooling experiment proposed for the BNL D2 line in 1995.

The 1995 proposal was not carried beyond the stage of a Letter of Intent, in part because of lack of definition of the overall cooling R&D program for a muon collider.

5 References

[1] G.K. O'Neill, *Storage-Ring Synchrotron: Device for High-Energy Physics Research*, Phys. Rev. **102**, 1418 (1956).

[2] D.B. Lichtenberg, P. Stehle and K.R. Symon, *Modification of Liouville's Theorem Required by the Presence of Dissipative Forces*, MURA Report 126 (July 12, 1956), http://puhep1.princeton.edu/mumu/physics/symon/1.html
A.A. Kolomensky, *On the Oscillation Decrements in Accelerators in the Presence of Arbitrary Energy Losses*, Sov. Atomic Energy **19**, 1511 (1965), http://puhep1.princeton.edu/mumu/physics/kolomensky/1.html
G.I. Budker, *An Effective Method of Damping Particle Oscillations in Proton and Antiproton Storage Rings*, Sov. Atomic Energy **22**, 438 (1967), http://puhep1.princeton.edu/mumu/physics/budker/1.html
Yu.M. Ado and V. I. Balbekov, *Use of Ionization Friction in the Storage of Heavy Particles*, Sov. Atomic Energy **31**, 731 (1971), http://puhep1.princeton.edu/mumu/physics/ado/1.html
V.I. Balbekov, *Achievable Transverse Emittance of Beam in Muon Collider*, AIP Conf. Proc. **372**, 140 (1996), ftp://ftp.mumu.bnl.gov/pub/documents/balbekov.ps

[3] C.M. Ankenbrandt *et al.*, *Status of muon collider research and development and future plans*, Phys. Rev. ST Accel. Beams **2**, 081001 (1999), http://prst-ab.aps.org/przv02i08tc.html
http://www.cap.bnl.gov/mumu/status_report.html

[4] B. Autin, A. Blondel, J. Ellis, eds., *Prospective Study of Muon Storage Rings at CERN*, (CERN 99-02, Apr. 30, 1999), http://preprints.cern.ch/cgi-bin/setlink?base=cernrep&categ=Yellow_Report&id=99-02

[5] K.T. McDonald, ed., *Expression of Interest for R&D towards A Neutrino Factory Based on a Storage Ring and a Muon Collider* (Nov. 7, 1999), http://puhep1.princeton.edu/~mcdonald/NSFLetter/nsfmain.ps

[6] D. Finley and N. Holtkamp, eds., *A Feasibility Study of a Neutrino Source Based on a Muon Storage Ring* (Mar. 31, 2000), http: www.fnal.gov/projects/muon_collider/nu-factory/

[7] P. Dendooven, *The development and status of the IGISOL technique*, Nucl. Instr. & Meth. **B126**, 182 (1997).

[8] R.B. Palmer, *Draft Parameters of a Neutrino Factory*, MUC0046 (updated Oct. 14, 1999), http://pubweb.bnl.gov/people/palmer/nu/params.ps

[9] R.C. Fernow *et al.*, *Possible demonstration of ionization cooling using absorbers in a solenoidal field*, A.I.P. Conf. Proc. **372**, 146 (1996).

[10] C.N. Ankenbrandt *et al.*, *Ionization Cooling Research and Development Program for a High Luminosity Muon Collider*, FNAL P904 (April 15, 1998); http://www-mucool.fnal.gov/mcnotes/muc0001.ps

[11] C. Lu, K.T. McDonald, E.J. Prebys and S.E. Vahsen, *A Detector Scenario for the Muon Cooling Experiment*, Princeton/$\mu\mu$/97-8 (May, 1998); http://puhep1.princeton.edu/mumu/mumu-97-8.ps

[12] K.T. McDonald, *Comments on Ionization Cooling*, Princeton/$\mu\mu$/98-17 (Feb. 10, 2000), http://puhep1.princeton.edu/mumu/coolingcom.ps

[13] D. Neuffer, *Principles and Applications of Muon Cooling*, Part. Acc. **14**, 75 (1983); reproduced in AIP Conf. Proc. **353**, 12 (1996).

[14] J. Norem, *X-Ray Measurements*, presented at the Neutrino Factory and Muon Collider Collaboration Meeting (LBL, Dec. 14, 1999).

[15] M.S. Zisman, *Neutrino Factory and Muon Collider Collaboration R&D Program: Present and Future*, presented at the Muon Collider Technical Advisory Committee review (BNL, June 15-16, 2000), http://pubweb.bnl.gov/people/gallardo/mutac_2000/zisman.ps

[16] S. Geer, *MUCOOL: Overview and Plans*, presented at the Muon Collider Technical Advisory Committee review (BNL, June 15-16, 2000), http://pubweb.bnl.gov/people/gallardo/mutac_2000/geer2.ps

[17] R.B. Palmer, C. Johnson, E Keil, *A Cost-Effective Design for a Neutrino Factory* (Nov. 25, 1999), http://www-mucool.fnal.gov/mcnotes/muc0067.ps

[18] *Muon Source Mini-Workshop* (TRIUMF, Mar. 24-25, 2000), http://sitka.triumf.ca/doug/prism_workshop/

[19] *Muon to Electron Conversion Experiment (MECO)*, BNL E940, http://meco.ps.uci.edu/

[20] *Precision Measurement of the Michel Parameters of μ^+ Decay*, TRIUMF E614, http://stoney.phys.ualberta.ca/~rodning/E614/

[21] J.S. Alcorn *et al.*, *The SLAC Two-Meter-Diameter, 25-Kilogauss, Superconducting Solenoid "Uamh Binn"*, Proceedings of the 1972 Applied Superconductivity Conference (May 1972), p. 273;
D. Aston *et al.*, *The LASS Spectrometer*, SLAC-R-298 (April 1987), http://www.slac.stanford.edu/pubs/slacreports/slac-r-298.html

[22] A.V. Tollestrup, *Kinematics and cross section for μe scattering*, MUC0016, http://www-mucool.fnal.gov/mcnotes/muc0016.ps

[23] A.V. Tollestrup, *Moliere Theory for 186 MeV/c Muons in Hydrogen*, MUC0020, http://www-mucool.fnal.gov/mcnotes/muc0020.ps

[24] A.V. Tollestrup, *R&D for MUCOOL*, MUC0089 (Feb. 1, 2000), http://www-mucool.fnal.gov/mcnotes/muc0089.ps

[25] P. Lebrun, *Modeling of Multiple Scattering Effects in Presence of a Strong Magnetic Field* MUC0030 (Oct. 20, 1999),
http://www-mucool.fnal.gov/mcnotes/muc0030.ps

[26] K.T. McDonald, *An Emittance Diagnostic Channel for R&D on the Front End of a Muon Collider/Neutrino Factory*, MUC0039;
http://puhep1.princeton.edu/mumu/diagnostic.ps

[27] D.J. Summers *et al.*, *Čerenkov Particle ID Status*, presented at the Neutrino Factory and Muon Collider Collaboration Meeting (LBL, Dec. 14, 1999). Figure 6 was provided by L. Cremaldi.

[28] Particle Data Group, *Review of Particle Properties*, Eur. Phys. J. C **3**, 1 (1998), p. 138;
http://pdg.lbl.gov/

[29] J.D. Jackson, *Classical Electrodynamics*, 2nd ed. (Wiley, New York, 1975), sec. 13.3. The discussion of straggling was omitted in the 3rd edition.

[30] H. Wiedemann, *Particle Accelerator Physics II* (Springer, Berlin, 1995).

[31] K.W. Robinson, *Radiation Effects in Circular Electron Accelerators*, Phys. Rev. **111**, 373 (1958).

[32] R.B. Palmer, D.V. Neuffer and J. Gallardo, *A Practical High-Energy High-Luminosity $\mu^+\mu^-$ Collider*, AIP Conf. Proc. **335**, 635 (1995).